



ALMA MATER STUDIORUM
UNIVERSITÀ DI BOLOGNA

ARCHIVIO ISTITUZIONALE
DELLA RICERCA

Alma Mater Studiorum Università di Bologna Archivio istituzionale della ricerca

Unsupervised analysis of background noise sources in active offices

This is the final peer-reviewed author's accepted manuscript (postprint) of the following publication:

Published Version:

De Salvo D., D'Orazio D., Garai M. (2021). Unsupervised analysis of background noise sources in active offices. THE JOURNAL OF THE ACOUSTICAL SOCIETY OF AMERICA, 149(6), 4049-4060 [10.1121/10.0005129].

Availability:

This version is available at: <https://hdl.handle.net/11585/835569> since: 2024-09-06

Published:

DOI: <http://doi.org/10.1121/10.0005129>

Terms of use:

Some rights reserved. The terms and conditions for the reuse of this version of the manuscript are specified in the publishing policy. For all terms of use and more information see the publisher's website.

This item was downloaded from IRIS Università di Bologna (<https://cris.unibo.it/>).
When citing, please refer to the published version.

(Article begins on next page)

Unsupervised analysis of background noise sources in active offices

Domenico De Salvio,¹ Dario D'Orazio,¹ and Massimo Garai¹

Department of Industrial Engineering (DIN), University of Bologna,

Viale Risorgimento 2, 40136 Bologna, Italy^a

1 Inside open-plan offices, background noise affects the workers' comfort, influencing
2 their productivity. Recent approaches identify three main source categories: mechan-
3 ical sources (HVAC equipment, office devices, etc.), outdoor traffic noise, and human
4 sources (speech). While the first two groups are taken into account by technical
5 specifications, human noise is still often neglected. The present paper proposes two
6 procedures to identify the human and mechanical noise sources during working hours,
7 based on machine-learning techniques. Two unsupervised clustering methods, specif-
8 ically Gaussian Mixture Model and K-means, were used to separate the recorded
9 sound pressure levels recorded finding the candidate models. Thus, the clustering
10 validation was used to find the number of sound sources within the office and then,
11 statistical and metrical features were used to label the sources. The results were
12 compared with the common parameters used in noise monitoring in offices, i.e. the
13 equivalent continuous and the 90th percentile levels. The spectra obtained by the two
14 Algorithms match with the expected shapes of human speech and mechanical noise
15 tendencies. The outcomes validate the robustness and reliability of these procedures.

^adario.dorazio@unibo.it

16 I. INTRODUCTION

17 Different kinds of noise can affect the individual perception, depending on personal fac-
18 tors (Ellermeier *et al.*, 2001), on the task to do (Braat-Eggen *et al.*, 2019), and on the nature
19 of the noise source (Koskela *et al.*, 2014). To ensure a more comfortable workspace, it is
20 important to take into account which work tasks are performed, the spatial distribution of
21 the workstations and the balance between ease of communication and concentration (Per-
22 rin Jegen and Chevret, 2017). In many cases, distraction in the work place is not strictly
23 related to the sound pressure level but more to the effect of irrelevant sound (Ellermeier
24 and Zimmer, 2014; Jones, 1999). In this latter case, the most distracting noise is due to
25 speech and the unintentional listening of the workmates conversations (Braat-Eggen *et al.*,
26 2019; Hongisto, 2005). The perception of mechanical noise has been investigated by clas-
27 sifying its characteristics (Iannace *et al.*, 2018). In some cases, this kind of noise sources
28 could even increase performance (Alimohammadi and Ebrahimi, 2017). These instances are
29 faced by acoustic consultants, who should balance the acoustic absorption inside open plan
30 offices while keeping the background noise at a reasonable level, because it is fundamental
31 to guarantee a low speech intelligibility (Di Blasio *et al.*, 2019; Schlittmeier and Liebl, 2015).

32 The spatial distribution of Speech Transmission Index (STI) was proved to be a work-
33 ers' performance metrics (Hongisto, 2005). The STI depends on the acoustical quality of
34 the room and on the background noise, even if international regulations on open-plan of-
35 fice acoustic quality (ISO 3382, 2012) state that STI must be evaluated by neglecting the
36 contribution of human noise. This condition that tends to underestimate the real acoustic

37 environment (Harvie-Clark *et al.*, 2019). It implies the assumption that the most distracting
38 situation is due to a single talker and not to a multi-talker scenario (Yadav and Cabrera,
39 2019; Yadav *et al.*, 2017). It is based on the fact that measurements in an unoccupied con-
40 dition are much more easily performed, when the role of the human activities involved in
41 background noise can be neglected. Consequently, it is neglected also during the evaluation
42 of the acoustic parameters. Open plan offices constitute dynamic scenarios in which people
43 are no longer to be considered only as sensitive receivers but also as sound sources them-
44 selves (Renz *et al.*, 2018a,b). A more specific background noise condition can be selected
45 to post-processing the STI values, so, in light of this, the measurement of this parameter
46 is crucial (D’Orazio *et al.*, 2018; Rindel, 2018). Different criteria have been proposed with
47 the aim to produce an objective descriptor of an acoustic environment, that enables people
48 to estimate its impact on their comfort and productivity (Renz *et al.*, 2019; Vellenga *et al.*,
49 2017).

50 In the field of room acoustics, data-analysis based techniques (Bianco *et al.*, 2019) were
51 used to measure the background noise due to human activity into classrooms (D’Orazio *et al.*,
52 2020; Hodgson *et al.*, 1999) and - in a preliminary way - in open plan offices too (Dehlbæk
53 *et al.*, 2016).

54 The aim of this work is to identify the sound sources via an unsupervised statistical
55 analysis of long-term monitoring, including the number of sources, their origin and the
56 sound pressure level they produce. The data population obtained from the recording done
57 with a sound level meter can be processed with algorithms used in unsupervised learning to
58 find pattern and create clusters. Then, each sound source can be reliably associated to each

59 cluster. In particular, machine learning techniques can help in precisely delineating human
60 noise. The results of the algorithms are compared with standard procedures to measure
61 background noise.

62 II. SOUND SOURCE DETECTION THROUGH DATA ANALYSIS

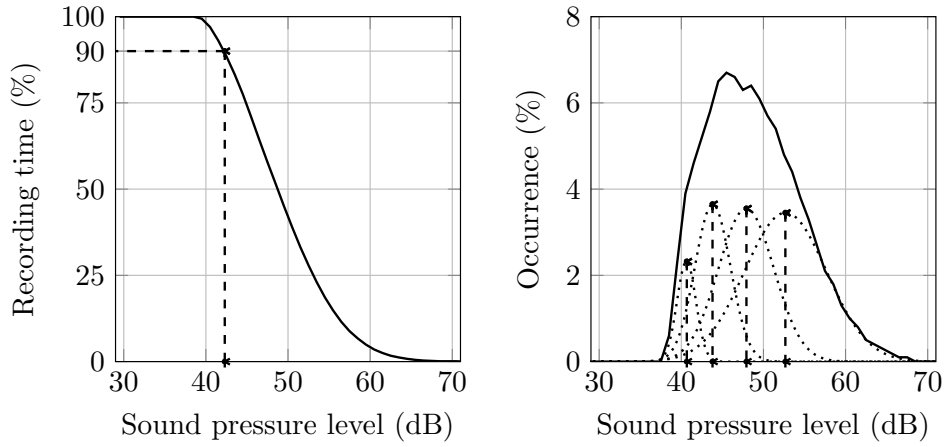
63 In the field of open-plan office acoustics, noise monitoring is often made with percentile
64 levels. Several thresholds of percentiles are used, often compared with the equivalent contin-
65 uous level L_{eq} . Vellenga-Persoon et al. used L_5 in the so called “liveliness ratio” (Vellenga
66 *et al.*, 2017), whereas percentiles L_5 , L_{10} , L_{90} , and L_{95} were compared by Renz et al. (Renz
67 *et al.*, 2019).

68 This kind of approach requires either the knowledge of the distribution of the occurrences
69 of the sound levels in the environment during monitoring time, or a supervision by the
70 operator. For these reasons, unsupervised algorithms can represent a useful tool for accurate
71 monitoring without the need of human supervision.

72 A. Clustering algorithms

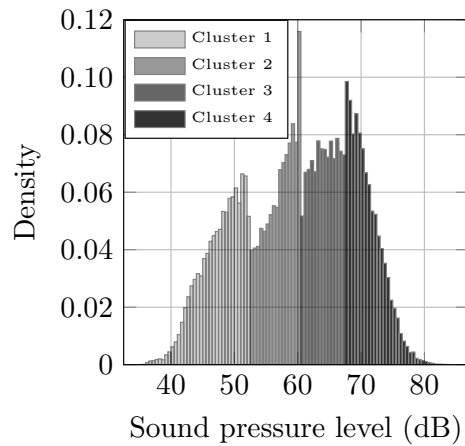
73 Clustering algorithms allow to identify different candidate noise sources by analyzing the
74 data collected from a recording. In this section, the Gaussian Mixture Model (GMM) and
75 the K-Means Clustering (KM) are introduced.

76 GMM is a clustering method which decomposes the original model data in a sum of
77 gaussian curves. Assuming a set of observations x_1, \dots, x_n (e.g. the short-time equivalent
78 levels recorded), the Gaussian probability density function $f(x_i)$ of these observations – in



(a) Percentile levels

(b) Gaussian Mixture Model



(c) K-means clustering

FIG. 1. The three unsupervised methods used in this work. In figure (a) the continuous line represent the cumulative distribution of the recorded SPL of a sound level meter and the * corresponds to the 90th Percentile Level L_{90} . In figure (b) the continuous line represents the occurrences distribution of the same measurement. The asymmetrical distribution can be decomposed in four Gaussian curves. The mean values of Gaussian curves indicated with * correspond to the sound levels attributed to each sound source. In figure (c) the four histograms represent four different clusters obtained via K-means clustering.

79 the following called *target density* – can be expressed as a sum of K Gaussian densities

80 $f_k(x_i, \mu_k, \sigma_k^2)$:

$$f(x_i) \simeq \sum_{k=1}^K \pi_k f_k(x_i, \mu_k, \sigma_k^2) \quad (1)$$

where π_k are the so called *mixing proportions* (McLachlan, G.J. and Peel, D., 2000), non-negative quantities that sum to one; that is,

$$0 \leq \pi_k \leq 1 \quad (k = 1, \dots, K)$$

and

$$\sum_{k=1}^K \pi_k = 1.$$

81 The likelihood function for a mixture model with K univariate Normal components is:

$$\mathcal{L}(x) = \prod_{i=1}^n \sum_{k=1}^K \pi_k f_k(x_i) = \prod_{i=1}^n \sum_{k=1}^K \pi_k \frac{1}{\sqrt{2\pi\sigma_k^2}} e^{-\frac{(x_i - \mu_k)^2}{2\sigma_k^2}}. \quad (2)$$

82 The equality in 1 is usually realized by maximum likelihood optimization algorithm, e.g.
83 the Expectation-Maximization (EM) (Dempster *et al.*, 1977). In the context of background
84 noise in open-plan offices, Dehlbaek *et al.* (Dehlbaek *et al.*, 2016) proposed a preliminary
85 analysis based on GMM. The probability distribution function of equivalent levels recorded
86 in several offices is fitted with one or more Gaussian curves. The means a Gaussian curve
87 is taken as the sound pressure levels of a sound source. If two normal curves are used,
88 then the higher mean is identified as human activity and the lower one as the background
89 noise in the office. The contribution of human activity is taken into account only if the
90 10th statistical percentile of the corresponding curve is greater than the background noise
91 measured in unoccupied condition.

92 While GMM is based on statistical properties of the data population, KM optimizes a
 93 metric distance of each single point data to form clusters. The set of observations x_1, \dots, x_n
 94 can be clustered into a set of K clusters, $C = \{c_k; k = 1, \dots, K\}$, where μ_k is the mean
 95 of cluster c_k . The squared Euclidean distances between μ_k and the points in cluster c_k is
 96 defined as:

$$J(c_k) = \sum_{x_i \in c_k} \|x_i - \mu_k\|^2. \quad (3)$$

97 The goal of K-means is to minimize the sum of the squared Euclidean distances over all K
 98 clusters:

$$J(C) = \sum_{k=1}^K \sum_{x_i \in c_k} \|x_i - \mu_k\|^2. \quad (4)$$

99 The process converges to a local minimum in two steps: first, the optimal partition for a
 100 given set of μ_k is found; then, the cluster centroids are computed once C is fixed (Lloyd,
 101 1982). A K-means clustering was preliminary used by Wang and Brill to monitor the noise
 102 levels in occupied and unoccupied conditions in several K-12 classrooms (Wang *et al.*, 2020).

103 B. Clustering validation

104 Clustering algorithms may produce redundant results, i.e. a number of clusters greater
 105 than the number of actual sound sources. Indeed, the maximum likelihood principle results
 106 in selecting the highest possible dimension (Schwarz, 1978). The clustering validation allows
 107 to assess the best model among candidates through specific metrics. In this work the Akaike
 108 Information Criterion (AIC) (Akaike, 1974) and the silhouette method (Rousseeuw, 1987)
 109 have been used to assess the optimal number of clusters for, respectively, GMM and KM.

110 AIC provides an assessment based on a reward for the goodness of fit to help in choosing

111 the best candidate as well as a penalization for the complexity of the model. Assuming k
112 as the number of estimated parameters in the model and \mathcal{L} the likelihood function defined
113 above, the AIC is:

$$AIC = 2k - 2 \ln [\mathcal{L}(x)]. \quad (5)$$

114 The first term of eq. 5 is the penalization of the complexity, whereas the second term concerns
115 the goodness of the fit. Thus, the greater the likelihood the lower the AIC. It follows that
116 the lowest value indicates the best model. Plotting the AIC obtained with different values
117 of K , the elbow of the curve highlights the optimal number of clusters. More in detail, the
118 AIC coefficient estimates the error caused by the loss of information due to the statistical
119 modelling of the initial data (Rodríguez, 2005). Instead of other information criteria like
120 the Bayesian information criterion (BIC), the AIC assumes that all the candidate models
121 are wrong, i.e. none of them is the true model that generated the data. Thus, the BIC
122 seeks the true model, which is the most probable, whereas the AIC seeks the wrong model
123 with the lowest loss of information, which is the most predictive referred to the initial data.
124 Moreover, it has been shown that AIC performs better than other information criteria when
125 the models are non-nested, i.e. one model is not a particular case of another (Gabbay *et al.*,
126 2011). The AIC has been chosen in the present work since all the candidate models are
127 assumed wrong and non-nested.

128 The silhouette method is a quantitative assessment of the degree of separation among
129 the clusters. Assuming i as a data point in the cluster A_m , the mean distance between i and
130 the other data points in the same cluster, is:

$$a(i) = \frac{1}{|A_m| - 1} \sum_{i,j \in A_m, i \neq j} d(i, j) \quad (6)$$

131 where $d(i, j)$ is the distance between i and j in the cluster A_m .

132 Thereafter, the mean dissimilarity of i to another cluster B_n is defined as the mean
 133 distance between i and the other points l in B_n . Thus:

$$b(i) = \min \frac{1}{|B_n|} \sum_{l \in B_n, l \neq i} d(i, l) \quad (7)$$

134 is the shortest mean distance between i and all the other points in the other clusters. Of
 135 course, this is possible only with a number of clusters $K > 1$. The cluster with the smallest
 136 mean dissimilarity is defined as “neighbor” and represents the second-best choice for i . The
 137 silhouette value $s(i)$ is defined as:

$$s(i) = \begin{cases} 1 - a(i)/b(i) & \text{if } a(i) < b(i), \\ 0 & \text{if } a(i) = b(i), \\ b(i)/a(i) - 1 & \text{if } a(i) > b(i). \end{cases} \quad (8)$$

138 Thus $-1 \leq s(i) \leq 1$, which means that i is properly clustered if $s(k)$ is near 1, while it is
 139 wrongly clustered if $s(i)$ is near -1, whereas an $s(i)$ near 0 means that i can be assigned to
 140 either A or B . The silhouette values $s(i)$ expresses how each data point is well clustered.
 141 Hence, the mean of each silhouette value of clusters $\bar{s}(i)$ can be considered as a metric for
 142 the whole clustering process. The silhouette coefficient SC, then is defined as:

$$SC = \max_k \bar{s}(k) \quad (9)$$

143 where k is the number of clusters. The silhouette coefficient, as well as being one of the most
144 well-known clustering validation indices, is assessed as very viable among different kinds of
145 dataset ([Jauhiainen and Kärkkäinen, 2017](#)).

146 **III. METHOD**

147 **A. Checking through 1-day recordings**

148 In order to evaluate the performance of the two methods, an office with four workstations
149 was chosen as test room.

150 The office is placed in a building away from the city center and road traffic. This means
151 that the expected soundscape involves only two main noise sources: human activity and
152 mechanical systems. Moreover, the room has an acoustically treated ceiling and thus, it
153 can be considered as a “dead” environment. Hence, the goal is to identify these two sound
154 sources during work hours. This test office, given the above mentioned simplifications,
155 allows to monitor the appropriate noise sources: human activity of several people at the
156 same time, mechanical noise due to air conditioning systems (which could be switched off
157 during measurements) and other office devices. The workplace layout is made up of four
158 workstations (ws A, ws B, ws C and ws D) and a meeting table. Despite the small size of
159 the office, the meeting table is far enough from the workstations to allow the analysis of
160 speech at the position number 4 (in figure 2).

161 Sound pressure levels monitoring was carried out throughout an entire working day, so to
162 allow to record enough data ([ISO 22955, 2020](#)). A statistical data population was obtained by

163 recording short-time equivalent levels, 100 ms integration time, octave-band filtered (125 Hz
164 - 4000 Hz), for an amount of time long enough to validate the central limit theorem.

165 Thereafter, the collected data were processed through the procedures shown in the fol-
166 lowing section. Furthermore, equivalent continuous L_{eq} , and percentile levels (L_{90} , L_{50} , and
167 L_{10}) were extracted in order to compare the results with previous studies on this topic ([Renz](#)
168 *et al.*, 2019).

169 **B. Description of the three-steps procedures**

170 The unsupervised analysis proposed here is based on two Algorithms. Algorithm 1 per-
171 forms the clustering via GMM and AIC. Algorithm 2 performs the clustering via KM and
172 silhouette. Both Algorithms act in three steps:

- 173 1. Preliminary clustering analysis, finding several numbers of candidate noise sources.
- 174 2. Selection of the best candidate through clustering validation.
- 175 3. Final clustering analysis and association of each cluster to a noise contribute on the
176 basis of statistical (Algorithm 1) or temporal (Algorithm 2) conditions.

177 In Algorithm 1, the first step performs the clustering via GMM. The procedure has been
178 repeated with a variable number of clusters $k = 1, \dots, 10$. The EM algorithm returns the
179 mean μ_k , the standard deviation σ_k , and the mixing proportions π_k of the each Gaussian
180 curve (see eqs. 1 and 2). In order to achieve meaningful results, EM algorithm is initialized
181 by means of the components, the covariance matrices, and the mixing proportions. An
182 option has been set in order to replicate the algorithm several times starting from different

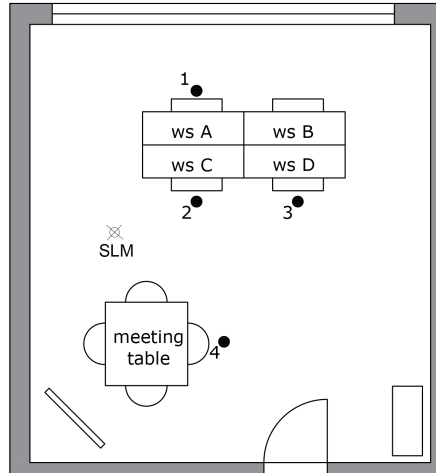


FIG. 2. Layout of the office with four workstations and a meeting table. The measurement positions (1 - 4) were used to evaluate the STI values and the role of irrelevant speech. The sound level meter, used for the long-time monitoring was placed between the workstations and the meeting table.

Algorithm 1: GMM and AIC

Input: x_i short-time levels octave-band filtered, $f(x_i)$ target distribution

Output: L_{human} ; L_{mech}

```
1 init EM
2 init  $L_{\text{mech}}, L_{\text{human}} = -\infty$ 
3 // first step
4 for  $k = 1 : 10$  do
5      $(\pi_k, \mu_k, \sigma_k) = \text{EM}(k, x_i)$ 
6 end
7 // second step
8 for  $k = 1 : 10$  do
9      $AIC(k) = 2k - 2 \ln(\mathcal{L}(\pi_k, \mu_k, \sigma_k; f(x_i)))$ 
10 end
11  $E = \text{elbow}(AIC(k))$ 
12 // third step
13  $(\pi_j, \mu_j, \sigma_j) = \text{EM}(E, x_i)$ 
14 for  $j = 1 : E$  do
15     if statistical condition then
16          $L_{\text{human}} = 10 \log(10^{\mu_j/10} + 10^{L_{\text{human}}/10})$ 
17     end
18     else
19          $L_{\text{mech}} = 10 \log(10^{\mu_j/10} + 10^{L_{\text{mech}}/10})$ 
20     end
21 end
```

Algorithm 2: KM and Silhouette

Input: x_i short-time levels octave-band filtered, $f(x_i)$ target distribution

Output: L_{human} ; L_{mech}

```
1 init KM
2 init  $L_{\text{mech}}, L_{\text{human}} = -\infty$ 
3 // first step
4 for  $k = 1 : 10$  do
5      $c_k = \text{KM}(k, x_i)$ 
6 end
7 // second step
8 for  $k = 2 : 10$  do
9      $s(k) = \text{Silhouette}(c_k; f(x_i))$ 
10 end
11  $A = k : \max_k (s(k))$ 
12 // third step
13  $c_j = \text{KM}(SC, x_i)$ 
14 for  $j = 1 : SC$  do
15     if metrical condition then
16          $L_{\text{human}} = 10 \log (10^{\text{centroid}(c_j)/10} + 10^{L_{\text{human}}/10})$ 
17     end
18     else
19          $L_{\text{mech}} = 10 \log (10^{\text{centroid}(c_j)/10} + 10^{L_{\text{mech}}/10})$ 
20     end
21 end
```

183 points, then the maximum likelihood is fitted. A covariance matrix of diagonal type is set,
184 whereas the mixing proportions are used with default parameters, which means that the
185 initial values are uniform. In the second step of Algorithm 1, the optimal number of clusters
186 is investigated through the AIC calculation according to equation 5. The goodness of fit
187 is rewarded through the likelihood function and, at the same time, the model is penalized
188 if it exceeds in complexity. The number k corresponding to the elbow of the curve is used
189 to perform again the GMM with the optimal number of clusters (see figure 3). Then, the
190 association among numerical and real sources existing within the office is made. Since in the
191 dataset used in the present study the traffic noise is negligible, in the third step of Algorithm
192 1 the way to discern the type of source was statistical. In fact, the standard deviation is
193 used as the parameter to distinguish the nature of the source, either mechanical or human.
194 It is expected that a low s.d. belongs to the mechanical sources, whereas a high s.d. to
195 human activity.

196 Instead, Algorithm 2 is based on KM and silhouette. The K-means clustering was set
197 using the square Euclidean distance as the metric to be minimized within the cluster c_k
198 and all over the k clusters (see eqs. 3 and 4). Then, as seen above for GMM, a specific
199 option to replicate the algorithm starting from different points was set to avoid the use of
200 the same centroids in the iterations. Also, Algorithm 2 was repeated with a variable number
201 of clusters $k = 2, \dots, 10$. Then, the silhouette method was used to choose the best model
202 among candidates. The mean values of the silhouettes of each cluster provides a metric to
203 evaluate the clustering goodness. Thus, the clustering validity is rated finding the highest
204 silhouette coefficient SC (equation 9) among candidate models, which means for various

205 number of clusters k , as described in the previous section. Then, KM is performed again
 206 with the optimal k . The subdivision between mechanical and human noise is based on a
 207 metrical hypothesis. The average distance of data points and the centroid within a cluster
 208 describes the density of clusters. A short distance can be associated to a mechanical source
 209 whereas a large value to human activity. The size of clusters can bring information about
 210 the frequency – in the temporal meaning – of the sound sources. For instance, a quiet office,
 211 with a low human activity within, will have a corresponding cluster with a large percentage
 212 of samples relative to the whole population.

213 C. Influence on Privacy-criteria

214 In order to evaluate the influence of background noise on the intelligibility of speech, a
 215 numerical model of the office was done using a ray tracing software to provide the mod-
 216 ulation transfer function of the room. The model was calibrated using the reverberation
 217 time measured in the office, assuming that the diffusivity conditions are met. This means
 218 that the calibration is achieved when the difference between the measured and simulated
 219 reverberation times lies within the just noticeable difference (JND), which is $\pm 5\%$, follow-
 220 ing the recommendations of the state-of-art (Vorländer, 2020). Once the model is set, the
 221 modulation transfer functions matrix (mtf) can be calculated from the simulated impulse
 222 response $h(t)$ for each k -th octave band and the modulation frequency f_m (IEC 60268, 2020):

$$m_k(f_m) = \frac{|\int_0^\infty h_k^2(t)e^{-j2\pi f_m t} dt|}{\int_0^\infty h_k^2(t) dt} \left[1 + 10^{-\frac{(L_{S,k} - L_{N,k})}{10}} \right]^{-1} \quad (10)$$

223 where $L_{S,k}$ is the useful speech level, which depends on the distance, and $L_{N,k}$ the background
224 noise. Through this matrix, the Speech Transmission Index can be calculated for each
225 workstation varying the background noise levels. Then, a predictive analysis of privacy
226 criteria within the active office can be carried out as function of the sound sources extracted.
227 This is very useful since it is directly linked to the studies about annoyance during work
228 hours (Ebisso *et al.*, 2015). Four positions were chosen as representative of the activity
229 performed inside the office: three near the workstations and one near the meeting table.
230 According to ISO 3382-3, the simulation of privacy criteria was carried out using a directional
231 sound source set at “normal” vocal effort. Different source-receiver configurations were
232 simulated by moving the source in one position (from n.1 to n.4) and the receivers in the
233 others. In order to calculate the matrix of the modulation transfer functions (mtf) for each
234 octave band (see equation 10), and then the speech transmission indices (STI), $L_{N,k}$ values
235 were set using the levels obtained by the Algorithms 1 and 2. In this way, it was possible
236 “to map” the speech privacy criteria for each source-receiver combination (Dickschen *et al.*,
237 2018).

238 IV. RESULTS

239 Tables I and II include the results of first step of clustering for both Algorithms. The
240 candidate noise sources are sought here. For Algorithm 1, this is achieved by looking for
241 the lowest AIC value in each octave band. Algorithm 2 is applied with the same number of
242 clusters used in Algorithm 1 in order to make a fair comparison. The standard deviations
243 of the Algorithm 1 are shown in brackets to have an overview of the clusters’ density.

244 The intermediate values achieved in the second step are shown in Figure 3. The clustering
245 evaluation metrics – AIC for Algorithm 1 and silhouettes for Algorithm 2 – assess the two
246 unsupervised techniques for a number of clusters K from 1 to 10 for AIC and 2 from
247 10 for silhouettes. Even though the analyses were carried out for K up to 10, the most
248 significant results are plotted up to $K = 6$ for a better visualization. $K = 2$ represents the
249 best candidate model for both metrics. For Algorithm 1, since AIC has an asymptotical
250 tendency, the elbow of the curves represents the reference for the best outcome. The 2 and
251 4 kHz octave bands reveal a slight change of slope between $K = 2$ and $K = 3$, but not
252 significant. For Algorithm 2, silhouettes show the high coefficients for $K = 2$ in each octave
253 band.

254 Then, the final outcomes produced by both Algorithms in the third step are shown in
255 Table III. Now the candidate sound sources are labeled as either mechanical or human,
256 on the basis of the above mentioned hypotheses (see Section IIIB). Bottalico and Astolfi
257 measured vocal doses of elementary male and female teachers finding an uncertainty of the
258 mean of the SPLs of about 4 dB (Bottalico and Astolfi, 2012). Olsen measured a standard
259 deviation of the mean of speech in the range of 4-6 dB (Olsen, 1998). Iannace et al. measured
260 the mechanical noise within an open-plan office in three operating conditions: two different
261 speeds and the background noise with the HVAC system off. The standard deviations in the
262 first two cases were about 1 dB, in the third was about 4 dB (Olsen, 1998). Leonard and
263 Chilton reported the measured ambient noise levels of previous studies in open-plan offices.
264 It is shown how the difference between minima and maxima SPLs span between 5 and
265 11 dB (Peter and Anthony, 2019).

266 Concerning the results of the present work, for Algorithm 1 the distinction is made setting
267 a standard deviation equal to 5 dB as threshold. If for a given sound source the standard
268 deviation is smaller than 5 dB, then this source is classified as mechanical, otherwise it
269 is associated to human activity. The standard deviations and the mixing proportions of
270 each Gaussian curve are shown in brackets. Regarding the Algorithm 2, the identification
271 is carried out analyzing the average distance of data points from the centroid within a
272 cluster. These distances and the size of clusters, represented as a percentage of the whole
273 data population, are shown in brackets. A short distance means a low spread of data points
274 within the cluster, which is referable to a mechanical source. A large distance highlights
275 a dynamic behaviour of the source, thus it is reasonable to associate this kind of source
276 to human activity. The clusters percentage breakout indicates that a large amount of data
277 belong to the mechanical source, on average 79% on the whole population. Consequently, the
278 office under study can be considered as a quiet environment. On the bottom of Table III, the
279 equivalent L_{eq} , and the percentile levels L_{90} , L_{50} , and L_{10} have been reported for comparison.

280 V. DISCUSSION

281 The office under study is located far from the city center in a quiet area, so indoor noises
282 were expected to be the main components of the monitored soundscape ([Acun and Yilmazer,](#)
283 [2018](#)). In particular, they are the noise due to service equipments and office devices, and
284 the human noise. The results of unsupervised analyses confirm this intuition: indeed the
285 clustering evaluation finds $K = 2$ as the best model among candidates. Now, it has to be
286 ascertained whether these numbers have a physical sense.

TABLE I. Results of the first step for Algorithm 1. Here, the candidate noise sources are sought. The results are obtained taking into account the lowest AIC possible. The standard deviations of the Gaussian curves are shown in brackets. All values are presented in dB for each octave band.

Frequency octave band (Hz)					
125	250	500	1000	2000	4000
Algorithm 1					
–	–	–	–	17.2 (0.4)	19.0 (0.4)
–	–	–	–	17.9 (0.3)	20.8 (0.3)
–	–	23.5 (1.2)	–	18.6 (0.4)	21.2 (0.2)
–	26.8 (1.4)	25.7 (1.1)	19.7 (1.0)	19.6 (0.6)	21.7 (0.2)
–	28.5 (1.0)	27.9 (1.0)	21.3 (0.8)	21.1 (0.9)	22.1 (0.3)
–	30.5 (1.0)	30.2 (1.1)	23.1 (1.1)	23.2 (1.2)	22.8 (0.7)
31.1 (1.9)	32.9 (1.4)	33.1 (1.7)	25.9 (1.9)	26.3 (1.7)	24.4 (1.6)
34.6 (3.3)	36.2 (2.6)	37.1 (2.9)	31.2 (3.9)	30.4 (3.0)	27.9 (3.2)
44.2 (6.9)	45.2 (6.8)	46.3 (7.9)	39.0 (8.3)	35.8 (7.1)	34.2 (6.0)

TABLE II. Results of the first step for Algorithm 2. Here, the candidate noise sources are sought. Algorithm 2 is applied with the same number of clusters set for Algorithm 1 in order to make a fair comparison. The average distances between each data point and the centroid within a cluster are shown in brackets. All values are presented in dB for each octave band.

Frequency octave band (Hz)					
125	250	500	1000	2000	4000
Algorithm 2					
–	–	–	–	17.8 (0.40)	20.6 (0.36)
–	–	–	–	19.9 (0.48)	21.8 (0.15)
–	–	23.9 (1.6)	–	22.6 (0.68)	23.4 (0.31)
–	27.0 (1.57)	27.8 (1.35)	20.6 (1.35)	25.7 (0.82)	25.7 (0.49)
–	30.6 (1.19)	32.0 (1.58)	24.3 (1.46)	28.9 (0.98)	28.3 (0.67)
–	34.6 (1.69)	36.5 (2.23)	29.0 (2.22)	32.5 (1.32)	31.4 (0.96)
31.3 (3.58)	39.8 (2.98)	42.4 (3.50)	34.7 (3.29)	36.8 (1.91)	35.2 (1.49)
37.7 (5.79)	46.8 (4.17)	49.5 (4.97)	42.0 (6.10)	42.2 (3.28)	40.0 (2.99)
49.6 (17.70)	54.0 (10.35)	58.0 (11.63)	52.1 (18.82)	49.8 (12.10)	47.7 (13.76)

TABLE III. Results of the third step for both Algorithms. The final outcomes associated to mechanical or human sources are shown. They are obtained running both Algorithms with $K = 2$, the optimal number of clusters found in the second step through the evaluation clustering (see Figure 3). For Algorithm 1, the standard deviations and the mixing proportions of the Gaussian curves of the Gaussian curves are shown, in brackets. For Algorithm 2, the average distances between each data point and the centroid within a cluster, and the size of each cluster expressed as percentage on the whole population, are shown, in brackets. Lastly, the equivalent and the 10th, 50th, and 90th percentile levels are shown for comparison. All values are presented in dB for each octave band.

Source type	Frequency octave band (Hz)					
	125	250	500	1000	2000	4000
Algorithm 1 – K=2						
Mech. (L_B)	32.5 (2.7 – 0.73)	30.0 (3.1 – 0.67)	28.1 (3.9 – 0.65)	22.2 (2.3 – 0.53)	18.6 (1.3 – 0.44)	21.6 (0.8 – 0.61)
Human (L_S)	41.6 (7.0 – 0.27)	41.3 (7.7 – 0.33)	40.7 (9.1 – 0.35)	32.5 (7.8 – 0.47)	28.0 (6.9 – 0.56)	27.5 (5.4 – 0.39)
Algorithm 2 – K=2						
Mech. (L_B)	32.7 (8.25 – 82%)	30.6 (11.75 – 79%)	28.6 (17.15 – 77%)	23.4 (10.16 – 75%)	20.3 (7.97 – 74%)	22.2 (3.01 – 84%)
Human (L_S)	45.5 (28.27 – 18%)	45.8 (31.65 – 21%)	45.8 (46.72 – 23%)	37.8 (40.45 – 25%)	33.7 (32.52 – 26%)	32.4 (21.11 – 16%)
L_{10}	42.9	45.4	45.5	37.7	34.0	30.0
L_{50}	33.3	31.7	30.3	24.6	21.3	22.1
L_{90}	29.5	26.7	23.7	19.9	17.5	20.7
L_{eq}	42.6	44.1	46.2	40.1	34.6	30.3

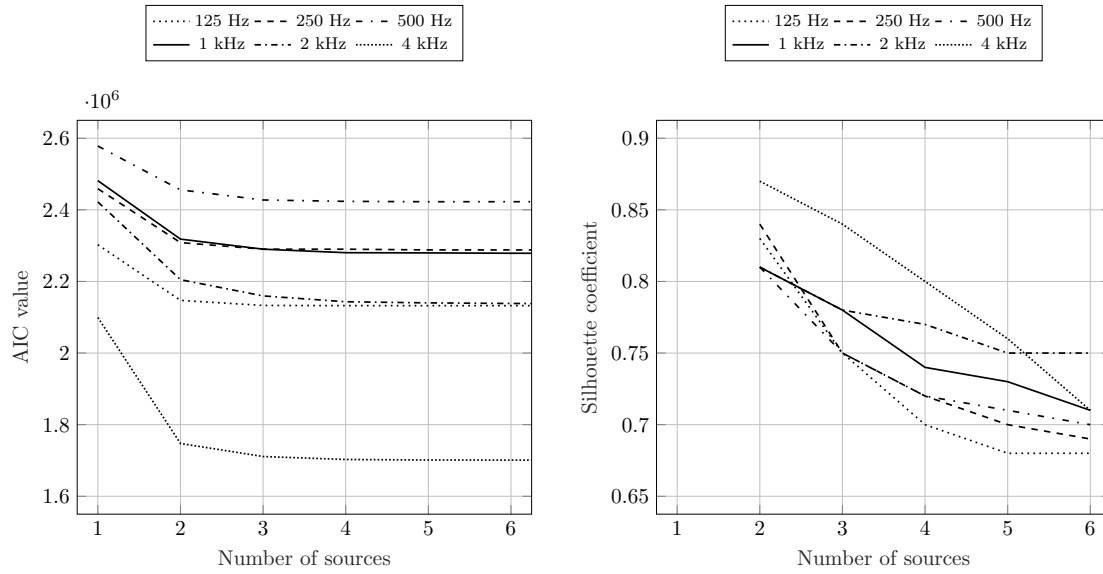


FIG. 3. Results of the second step for both Algorithms. AIC values on the top and silhouette evaluation on the bottom are shown for each octave band. The lower the AIC the better the model. The elbow of these curves represents the reference to evaluate the proper number of clusters to take into account in the analysis. Concerning the silhouettes, the higher the coefficient the better the model.

287 The two initial hypotheses used to identify the kind of source – i.e. mechanical or human
288 – are similar but have different concepts and applications. The continuous and constant
289 activity of the mechanical systems and devices is addressed with two different approaches:
290 the statistical occurrences in Algorithm 1, and the number of bins in Algorithm 2.

291 The unsupervised algorithms are able to detect different densities within the SPLs col-
292 lected by a sound level meter, regardless of its nature, mechanical or human. Finding the
293 centre of gravity, like means or centroids, implies the capability of quantifying the sources
294 in a dynamic context.

295 In the following, the results of both Algorithms will be compared from a statistical and
296 spectral point of view, respectively.

297 **A. Statistical remarks on the sound sources**

298 After finding the clusters, hence the active sound sources, it is necessary to label them,
299 i.e. to associate each cluster to an existing sound source. The statistical approach of
300 Algorithm 1 has more features to investigate in order to find the metrics and describe the
301 nature of the source. The metrical approach of Algorithm 2 needs to find similar metrics
302 in order to compare the results. In this regard, a small standard deviation means that the
303 associated sound source produces stable sound pressure levels continuously during time. It
304 is reasonable to associate this kind of behaviour to a mechanical source. In contrast, a high
305 standard deviation means a more accidental nature of the sound source, like human activity
306 ([Bottalico and Astolfi, 2012](#)). Similarly, a cluster shaped by a mechanical source should have
307 a high density of data points. This means a short average distance among the data points

308 and their centroid within the cluster. A more random source should have more spread sound
309 pressure levels, thus a lesser density and a larger average distance among data points and
310 the centroid. These considerations are confirmed by the fact that standard deviations from
311 Algorithm 1 and average distances of data points from Algorithm 2 have the same trend.
312 Moreover, the mixing proportions of clusters is quite similar as well. In fact, the absolute
313 values of the weight of each cluster take different values in the two Algorithms, but in both
314 methods the mechanical source has the higher weight. Just one exception is present, in the
315 2 kHz band.

316 GMM can be considered as a generalization of KM for very small variances ([MacKay,](#)
317 [2003](#)). The higher the variances the larger the differences between the values achieved by
318 Algorithm 1 and 2. Thus, this can be considered as a consequence of the heteroscedasticity
319 of data.

320 The large population of the recorded data seems to give more robustness to Algorithm
321 1. Concerning this point, in [Figure 4](#) the coefficients of variation, i.e. the ratio between the
322 standard deviations and the mean values, are plotted for each octave band and for the two
323 kind of sources, previously identified as mechanical and human. These coefficients show the
324 dispersion of the data distribution for Algorithm 1. The trend is the same up to the 500 Hz
325 octave band. Beyond this point, the gap between the curves of the mechanical and human
326 coefficients of variation increases. The spread of the human activity noise increases up to
327 the 2 kHz octave band: this source increases its dynamical behaviour in a range crucial for
328 the human speech, where most formants occur. In the 4 kHz band there is a change of
329

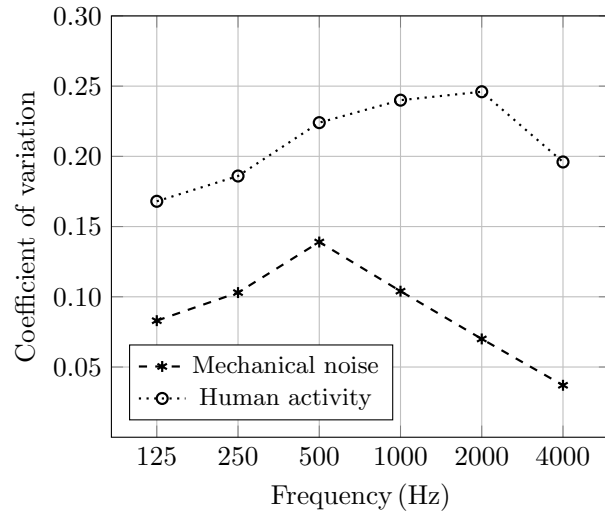


FIG. 4. Coefficient of variation of the two sources, the mechanical noise and the human activity, obtained by Algorithm 1. Results are plotted for each octave band.

330 tendency. So, this general trend supports the identification of the higher curve as belonging
331 to the human activity.

332 **B. Spectral remarks**

333 The human nature of the higher means and centroids resulting from the unsupervised
334 analysis can be confirmed by a spectral matching technique. Thus, the sound pressure levels
335 of speech in the office under study, was calculated using the diffuse field hypotheses and the
336 in situ measured values of reverberation time (Hodgson *et al.*, 2007). In fact, all the distances
337 among workstations are greater than the critical distance of the room. A talking time of
338 about the 20% of the whole monitoring time was considered. Because the background
339 noise levels, measured within the office, remain almost below 45 dB, the Lombard effect is
340 not triggered; this allows to use a constant value of speech power level (Peter and Anthony,
341 2019). The sound power level of normal speech has been set, according to the ISO 3382-
342 3, as an averaged value between male and female speakers and for a normal voice effort.
343 Taking into account recent findings, it is worth noting that the speech spectrum may change
344 in noisy environments, especially on lower bands (Leembruggen *et al.*, 2016; Rindel *et al.*,
345 2012). In light of this, the 125 and 250 Hz octave bands of the ISO speech spectrum have
346 been increased respectively of 6 and 3 dB. The SPLs calculated in this way were then
347 compared with the measured values of human noise obtained with Algorithm 1, Algorithm
348 2, and L_{eq} (see Figure 5). The human activity is not continuous in each recorded frame; it
349 represent just a percentage of time of the whole data population collected. In Figure 5 the
350 dashed curve refers to the expected speech spectrum.

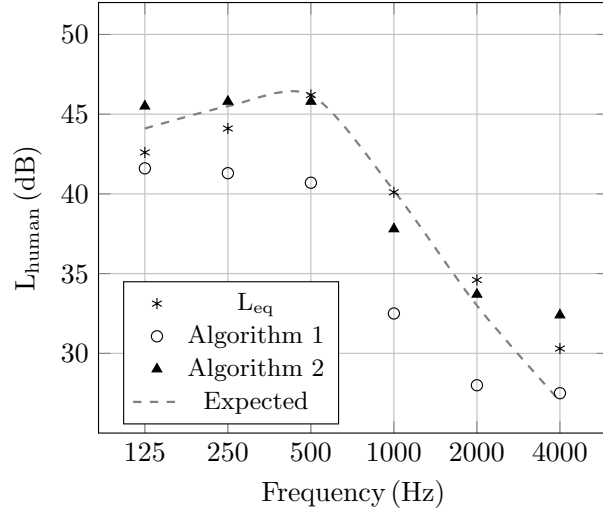


FIG. 5. Spectral matching between the calculated speech level in the room (under a diffuse sound field assumption; dashed line) and inferred values of the noise source identified as human using Algorithms 1 and 2 in the office under study. The dashed line is plotted assuming the speech running for the 20% of the monitoring time.

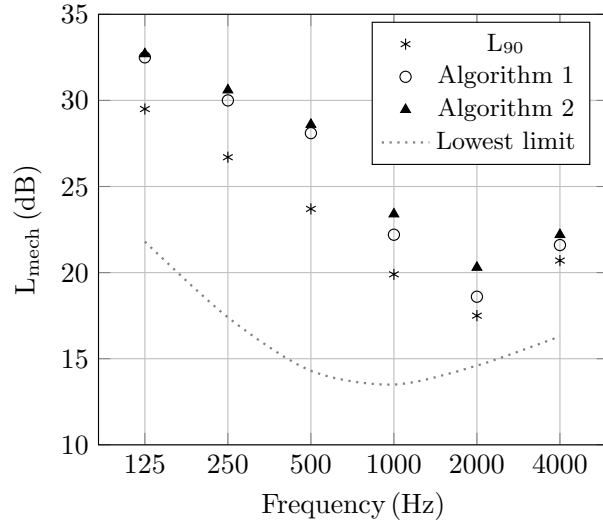


FIG. 6. Inferred values of the noise source identified as mechanical using Algorithms 1, Algorithm 2 compared with measured L_{90} in the office under study. The dotted curve shows the lowest detectable limit of the equipment used.

353 The qualitative analysis of the results shows how the detected human activity has a
354 similar spectrum of the calculated speech in the office. The quantitative analysis shows
355 differences among the methods. The Algorithm 1 gives significantly lower values compared
356 to other methods and the expected curve. This gap among values could concern the type of
357 classification of the clustering techniques. The GMM is defined as a soft clustering technique,
358 i.e. each data point is assigned to each cluster with different probabilities, whereas the KM
359 is an hard clustering technique, thus each data point can be assigned to one and only one
360 cluster (Saxena *et al.*, 2017). Thus, the overlap zone between two Gaussian curves obtained
361 by a mixture seems to lower the SPLs attributable to the source, corresponding to the mean
362 values of the Gaussian curves. The hard clustering performed by the Algorithm 2, seems
363 to process the classification similarly to the equivalent levels and the expected spectrum
364 calculated instead. The quite flat tendencies on lower frequencies obtained via Algorithms
365 1 and 2 could be due to the masking effects of the mechanical noise, which is louder in
366 this octave band, with respect to the few energy of the speech spectrum in these octave
367 bands. Such effect has been already noticed by (D’Orazio *et al.*, 2020). Nevertheless, the
368 flat tendency at the low frequencies falls within the uncertainties mentioned above.

369 Concerning Algorithm 1, this outcome can be led back to the low offset noticed in Fig-
370 ure 4. The separation in the lower band of 125 and 250 Hz seems to be more challenging,
371 maybe due to the high energetic contribution of both sources, mechanical and human. The
372 comparison between the mean values identified as human source and the diffuse speech levels
373 characteristic of the office under study shows the same trend with differences up to 4 dB.
374 This result confirms, with good approximation, the threshold chosen for the standard devi-

375 ation. Another confirmation of the reliability of the Algorithms 1 and 2 is obtained looking
376 at the clusters obtained by Algorithm 2. In fact, the average percentage over all the octave
377 band of the human activity is about 21% of the monitoring time (see Table III). This can
378 be assumed, in a first approximation, as the percentage of speech occurrence in the office
379 during work hours. Thus, the trend of the Algorithm 2, shown in Figure 5, seems to be the
380 more similar to the energetic model, since it is near the expected curve of the speech for the
381 20% of the whole monitoring time.

382 Moreover, in Fig. 6 the spectra of the mechanical noise obtained by Algorithms 1 and 2
383 and the 90th percentile levels are shown. The small differences between Algorithm 1 and
384 Algorithm 2, as stated in the previous section, can be explained as a consequence of the small
385 heteroscedasticity, and thus the low variances of the data, between the mechanical sources
386 obtained via GMM and KM. Moreover, the mechanical noise measured via Algorithms 1
387 and 2 has greater values than the 90th percentile level usually used.

388 An unforeseen tendency is presented by the 4000 Hz octave band in both spectra, me-
389 chanical and speech. In fact, it is expected a strong decrease of these values for both sources.
390 The dotted line represents the lowest limit detectable of the sound level meter used. Looking
391 at this and considering the high quiet of the office, the growth of the levels in the 4000 Hz
392 band of the mechanical spectrum, as well as the small decrease of this octave band in the
393 speech spectrum, can be given to the intrinsic error of the instrument. This observation
394 seems to be confirmed by the behaviour of the AIC and the silhouette coefficient of the 4000
395 Hz octave band shown in Figure 3. The large gap of the AIC value and the different ten-
396 dency of the silhouette coefficient, compared to the other octave bands, suggests a different

397 distribution of the SPLs within the database, hence imputable to the intrinsic noise of the
398 measurement.

399 C. Background noise correction for STI evaluation

400 A simulation of the office was done to obtain the STI values without background noise,
401 STI_{∞} , and then they were corrected with the background noise levels obtained with the two
402 Algorithms and the percentile levels (table III). STI values, corrected with the contribution
403 of mechanical and human noise separately, are shown in a source – receiver matrix (see
404 Figure 7) where the gray scale reveals the variation of the parameter: from 0.5 (in black),
405 which is the lower measured value, to 1 (in white), which is the ideal value of perfect
406 intelligibility achieved when source and receiver are in the same workstation. The correction
407 of STI_{∞} was made in two steps: at first, only the background noise due to the mechanical
408 sources has been considered; then the contribution of the human activity was added . In
409 figure 7 it is possible to see that there is a slight difference in the gray shade between the
410 first two matrices in a row and only in the third matrix, when both the types of noise are
411 considered, the shades are darker. For Algorithm 1, the variation of STI values is noticeable
412 when only the mechanical contribution or the human contribution is considered. These
413 results highlight that a more detailed analysis of the background noise allows to better
414 evaluate the variation of STI values, avoiding to overestimate this important quantity.

415 These results suggest how to assess the effective privacy condition within the office,
416 which is quite different than the privacy condition measured with the mechanical noise only,
417 as currently required by technical standards. In fact, the effective privacy is significantly

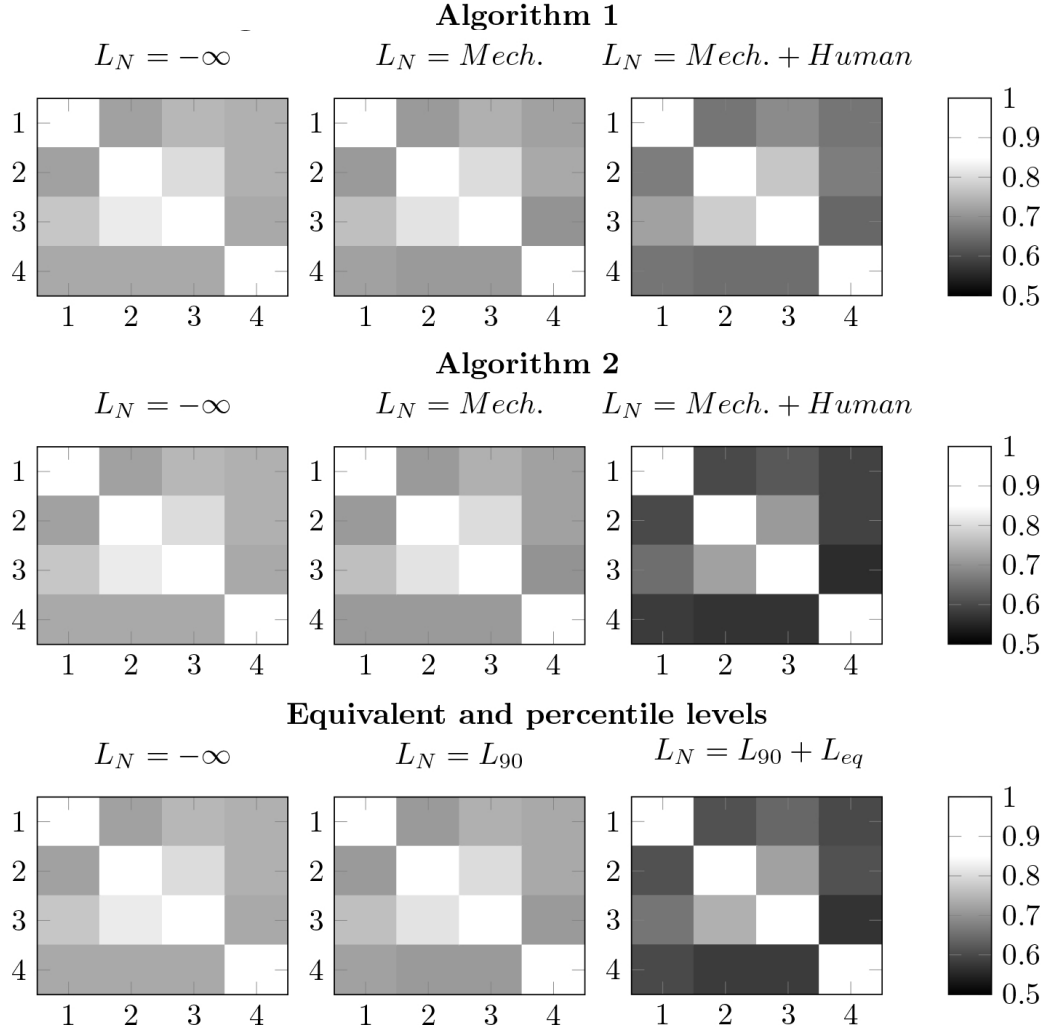


FIG. 7. Matrices of the STI values among the workstations in the office under study. The source has been set at the “normal” speech level. On each row, going from the left to right, the STI is presented first without background noise (indicated as $L_N = -\infty$), then corrected with the background noise levels obtained through the unsupervised analysis. First adding the mechanical contribution only (indicated as $L_N = L_{mech}$), then summing up the human contribution as well (indicated as $L_N = L_{mech} + L_{human}$). The sidebar on the right represents the legend of the STI values. On the axis of the matrix are reported the source-receiver positions (1 – 4) corresponding to the three workstations and the meeting table (see Figure 2).

418 affected by the social context (Rasmussen and Carrascal García, 2019). Where the active
419 noise masking is used, the speech privacy can be quite constant over the working areas.
420 In other cases, such as the one under study, the privacy fluctuates dynamically in time.
421 The results obtained with the procedure presented in this work allow to assess different
422 scenarios, thus broadening the characterization of privacy criteria of ISO 3382-3. Further
423 analyses could be done with these unsupervised Algorithms with longer monitoring times, in
424 order to investigate the existence of more significant correlations with percentile levels (Renz
425 *et al.*, 2019).

426 VI. CONCLUSIONS

427 Workers' comfort and productivity inside offices is influenced by the background noise,
428 which is due to different contributions (mechanical equipment, outdoor traffic, human ac-
429 tivity). Therefore it is highly desirable to be able to separate these contributions from the
430 temporal history provided by a simple monitoring systems. This would allow to control
431 HVAC noise during working hours or to dynamically optimize the speech privacy between
432 workers. Therefore, unsupervised algorithms capable to perform this task in an automated
433 manner are required. However, even if some procedures were proposed in previous research,
434 the instance seems to be still open. In the present work, two unsupervised methods capable
435 to separate and identify different noise sources from the same recording are described in
436 details. Both are based on clustering algorithms (GMM and K-Means) and further refined
437 by a clustering evaluation. The third step of each Algorithm may be adapted on the context
438 under study, on the basis of statistical and temporal preliminary observations.

439 The two Algorithms have been checked on a dataset of short-time (100 ms) equivalent
440 levels, coming from the recording of a whole working day in a small office. Two noise
441 sources, later identified as mechanical and human noise, were extracted from the dataset. It
442 has been shown how the candidates noise sources - extracted in the first step - were easily
443 reduced by the clustering evaluation. The Akaike information criterion and the silhouette
444 criterion were applied in each octave band, returning comparable results. It was noted that
445 Algorithm 1 is more sensitive to the statistical characteristics of the noise sources, while
446 Algorithm 2 is more sensitive to the temporal behavior. As a consequence, in the third step,
447 the proposed Algorithms return slightly different results. Indeed the two kind of noise sources
448 vary less (the mechanical one) or more (the human one) in time, so that the homoscedasticity
449 is not reached. Therefore, there are uncertainties at low frequencies, where the speech noise
450 energy is lower than the mechanical noise one. Increasing the frequency of the input signal,
451 the two sound sources seem to be identified by the statistical-based approach (Algorithm
452 1) better than by the metric-based approaches (Algorithm 2). Nevertheless, Algorithm 2
453 return information on the temporal behavior that are useful to optimize Algorithm 1, so
454 both of them seems to be needed for in a depth analysis.

455 With respect to previous researches, the unsupervised Algorithms presented here are
456 quite robust and, after a preliminary set, they could be implemented, e.g., in continuous
457 monitoring systems.

458 **ACKNOWLEDGMENTS**

459 The authors would like to thank Elena Rossi for the help during the preliminary research,
460 Giulia Fratoni for having set the numerical model, Laura Anderlucci for the useful hints on
461 the statistical analysis and Michele Ducceschi for the kind revision.

462

463 Acun, V., and Yilmazer, S. (2018). “A grounded theory approach to investigate the per-
464 ceived soundscape of open-plan offices,” *Applied Acoustics* **131**, 28–37.

465 Akaike, H. (1974). “A new look at the statistical model identification,” *IEEE transactions*
466 *on automatic control* **19**(6), 716–723.

467 Alimohammadi, I., and Ebrahimi, H. (2017). “Comparison between effects of low and high
468 frequency noise on mental performance,” *Applied Acoustics* **126**, 131–135.

469 Bianco, M. J., Gerstoft, P., Traer, J., Ozanich, E., Roch, M. A., Gannot, S., and Deledalle,
470 C.-A. (2019). “Machine learning in acoustics: Theory and applications,” *The Journal of*
471 *the Acoustical Society of America* **146**(5), 3590–3628.

472 Bottalico, P., and Astolfi, A. (2012). “Investigations into vocal doses and parameters per-
473 taining to primary school teachers in classrooms,” *The Journal of the Acoustical Society*
474 *of America* **131**(4), 2817–2827.

475 Braat-Eggen, E., vd Poll, M. K., Hornikx, M., and Kohlrausch, A. (2019). “Auditory dis-
476 traction in open-plan study environments: Effects of background speech and reverberation
477 time on a collaboration task,” *Applied Acoustics* **154**, 148–160.

478 Dehlbæk, T. S., Brunskog, J., Petersen, C. M., and Marie, P. (2016). “The effect of human
479 activity noise on the acoustic quality in open plan offices,” in *INTER-NOISE and NOISE-*
480 *CON Congress and Conference Proceedings*, Institute of Noise Control Engineering, Vol.
481 253, pp. 4117–4126.

482 Dempster, A. P., Laird, N. M., and Rubin, D. B. (1977). “Maximum likelihood from in-
483 complete data via the em algorithm,” *Journal of the Royal Statistical Society: Series B*
484 (Methodological) **39**(1), 1–22.

485 Di Blasio, S., Shtrepi, L., Puglisi, G. E., and Astolfi, A. (2019). “A cross-sectional survey
486 on the impact of irrelevant speech noise on annoyance, mental health and well-being, per-
487 formance and occupants’ behavior in shared and open-plan offices,” *International journal*
488 *of environmental research and public health* **16**(2), 280.

489 Dickschen, A., Bertazzoni, R., and Liebl, A. (2018). “Evaluating room acoustic quality in
490 open-plan offices by adding the distribution of possible source and receiver positions to the
491 simulation,” *Proceedings Euronoise 2018* 27–31.

492 D’Orazio, D., De Salvio, D., Anderlucci, L., and Garai, M. (2020). “Measuring the speech
493 level and the student activity in lecture halls: Visual-vs blind-segmentation methods,”
494 *Applied Acoustics* **169**, 107448.

495 D’Orazio, D., Rossi, E., and Garai, M. (2018). “Comparison of different in situ measure-
496 ments techniques of intelligibility in an open-plan office,” *Building Acoustics* **25**(2), 111–
497 122.

498 Ebissou, A., Parizet, E., and Chevret, P. (2015). “Use of the speech transmission index for
499 the assessment of sound annoyance in open-plan offices,” *Applied Acoustics* **88**, 90–95.

500 Ellermeier, W., Eigenstetter, M., and Zimmer, K. (2001). “Psychoacoustic correlates of
501 individual noise sensitivity,” *The Journal of the Acoustical Society of America* **109**(4),
502 1464–1473.

503 Ellermeier, W., and Zimmer, K. (2014). “The psychoacoustics of the irrelevant sound effect,”
504 *Acoustical Science and Technology* **35**(1), 10–16.

505 Gabbay, D. M., Thagard, P., Woods, J., Bandyopadhyay, P. S., and Forster, M. R. (2011).
506 *Philosophy of Statistics*, **7** (Elsevier).

507 Harvie-Clark, J., Larrieu, F., and Opsanger, C. (2019). “Iso 3382-3: Necessary but not suf-
508 ficient. a new approach to acoustic design for activity-based-working offices,” *Proceedings*
509 *of the 23rd International Congress on Acoustics* .

510 Hodgson, M., Rempel, R., and Kennedy, S. (1999). “Measurement and prediction of typical
511 speech and background-noise levels in university classrooms during lectures,” *The Journal*
512 *of the Acoustical Society of America* **105**(1), 226–233.

513 Hodgson, M., Steininger, G., and Razavi, Z. (2007). “Measurement and prediction of speech
514 and noise levels and the lombard effect in eating establishments,” *The Journal of the*
515 *Acoustical Society of America* **121**(4), 2023–2033.

516 Hongisto, V. (2005). “A model predicting the effect of speech of varying intelligibility on
517 work performance,” *Indoor air* **15**(6), 458–468.

518 Iannace, G., Ciaburro, G., and Trematerra, A. (2018). “Heating, ventilation, and air condi-
519 tioning (hvac) noise detection in open-plan offices using recursive partitioning,” *Buildings*
520 **8**(12), 169.

521 IEC 60268 (2020). “Sound System Equipment - Part 16: Objective rating of speech intelligi-
522 bility by speech transmission index” (International Electrotechnical Commission, Geneva,
523 Switzerland).

524 ISO 22955 (2020). “Acoustics - Acoustic quality of open office spaces” (International Orga-
525 nization for Standardization, Geneva, Switzerland).

526 ISO 3382 (2012). “Acoustics - Measurement of room acoustic parameters — part 3: Open-
527 plan offices” (International Organization for Standardization, Geneva, Switzerland).

528 Jauhainen, S., and Kärkkäinen, T. (2017). “A simple cluster validation index with max-
529 imal coverage,” in *European Symposium on Artificial Neural Networks, Computational*
530 *Intelligence and Machine Learning*, ESANN.

531 Jones, D. (1999). “The cognitive psychology of auditory distraction: The 1997 bps broad-
532 bent lecture,” *British Journal of Psychology* **90**(2), 167–187.

533 Koskela, H., Maula, H., Haapakangas, A., Moberg, V., and Hongisto, V. (2014). “Effect of
534 low ventilation rate on office work performance and perception of air quality—a laboratory
535 study,” *Proceedings of Indoor Air* 673–675.

536 Leembruggen, G., Verhave, J. *et al.* (2016). “The effect on sti results of changes to the male
537 test-signal spectrum,” *Proc IOA* **38**, 78–87.

538 Lloyd, S. (1982). “Least squares quantization in pcm,” *IEEE transactions on information*
539 *theory* **28**(2), 129–137.

540 MacKay, D. J. (2003). *Information theory, inference and learning algorithms* (Cambridge
541 university press).

542 McLachlan, G.J. and Peel, D. (2000). *Finite Mixture Models* (Wiley Series in Probability
543 and Statistics, New York).

544 Olsen, W. O. (1998). “Average speech levels and spectra in various speaking/listening con-
545 ditions,” *American Journal of Audiology* **7**, 21–25.

546 Perrin Jegen, N., and Chevret, P. (2017). “Effect of noise on comfort in open-plan offices:
547 application of an assessment questionnaire,” *Ergonomics* **60**(1), 6–17.

548 Peter, L., and Anthony, C. (2019). “The lombard effect in open plan offices,” in *Proceedings*
549 *of the Institute of Acoustics*, Institute of Acoustics, Vol. 41, pp. 216–226.

550 Rasmussen, B., and Carrascal García, T. (2019). “Acoustic regulations for offices-
551 comparison between selected countries in europe,” in *INTER-NOISE and NOISE-CON*
552 *Congress and Conference Proceedings*, Institute of Noise Control Engineering, Vol. 259,
553 pp. 8141–8150.

554 Renz, T., Leistner, P., and Liebl, A. (2018a). “Auditory distraction by speech: Can a bab-
555 ble masker restore working memory performance and subjective perception to baseline?,”
556 *Applied Acoustics* **137**, 151–160.

557 Renz, T., Leistner, P., and Liebl, A. (2018b). “Auditory distraction by speech: Sound
558 masking with speech-shaped stationary noise outperforms- 5 db per octave shaped noise,”
559 *The Journal of the Acoustical Society of America* **143**(3), EL212–EL217.

560 Renz, T., Leistner, P., and Liebl, A. (2019). “Use of energy-equivalent sound pressure levels
561 and percentile level differences to assess the impact of speech on cognitive performance
562 and annoyance perception,” *Applied Acoustics* **153**, 71–77.

563 Rindel, J. H. (2018). “Open plan office acoustics—a multidimensional optimization problem,”
564 Proceedings of DAGA2018, Munich, Deutsche Gesellschaft für Akustik .

565 Rindel, J. H., Christensen, C. L., and Gade, A. C. (2012). “Dynamic sound source for
566 simulating the lombard effect in room acoustic modeling software,” in *INTER-NOISE and*
567 *NOISE-CON Congress and Conference Proceedings*, Institute of Noise Control Engineering,
568 Vol. 2012, pp. 954–966.

569 Rodríguez, C. C. (2005). “The abc of model selection: Aic, bic and the new cic,” in *AIP*
570 *Conference Proceedings*, American Institute of Physics, Vol. 803, pp. 80–87.

571 Rousseeuw, P. J. (1987). “Silhouettes: a graphical aid to the interpretation and validation
572 of cluster analysis,” *Journal of computational and applied mathematics* **20**, 53–65.

573 Saxena, A., Prasad, M., Gupta, A., Bharill, N., Patel, O. P., Tiwari, A., Er, M. J., Ding,
574 W., and Lin, C.-T. (2017). “A review of clustering techniques and developments,” *Neuro-*
575 *computing* **267**, 664–681.

576 Schlittmeier, S. J., and Liebl, A. (2015). “The effects of intelligible irrelevant background
577 speech in offices—cognitive disturbance, annoyance, and solutions,” *Facilities* .

578 Schwarz, G. (1978). “Estimating the dimension of a model,” *Annals of statistics* **6**(2), 461–
579 464.

580 Vellenga, S., Bouwhuis, T., and Höngens, T. (2017). “Proposed method for measuring
581 ‘liveliness’ in open plan offices,” in *Proceedings of the 24th International Congress on*
582 *Sound and Vibration, London, UK*, pp. 23–27.

583 Vorländer, M. (2020). *Auralization* (Springer).

584 Wang, L. M., Brill, L. C., Nord, J., and Bovaird, J. (2020). “Higher speech levels in k-12
585 classrooms correlate with lower math achievement scores,” *The Journal of the Acoustical*
586 *Society of America* **148**(4), 2631–2632.

587 Yadav, M., and Cabrera, D. (2019). “Two simultaneous talkers distract more than one in
588 simulated multi-talker environments, regardless of overall sound levels typical of open-plan
589 offices,” *Applied Acoustics* **148**, 46–54.

590 Yadav, M., Kim, J., Cabrera, D., and De Dear, R. (2017). “Auditory distraction in open-
591 plan office environments: The effect of multi-talker acoustics,” *Applied Acoustics* **126**,
592 68–80.